Eurasian Journal of Physics and Functional Materials

2019, 3(2), 116-123

Isobaric resonances, beta decay and delayed multineutron emission in very neutron-rich nuclei

I.N. Borzov*,[1,2], S.V. Tolokonnikov[1]

[1]National Research Centre Kurchatov Institute, Moscow, Russia

[2]Joint Institute of Nuclear Research, Dubna, Russia

E-mail: borzov_in@nrcki.ru

DOI: **10.29317/ejpfm.2019030201**
Received: 25.04.2019 - after revision

The isobaric-analog resonancesfor nuclei around the neutron shell closures at N = 20, 50, 82 are treated in the fully self-consistent Density Functional plus Continuum Quasiparticle Random Phase Approximation (DF+CQRPA).The aim is to check how the self-consistency is preserved in the calculations for long isotopic chains. The beta-decay half-lives and delayed multi-neutron emission branchingare calculated for the reference Ni isotopic chain. The relative contributions of the GT and first-forbidden transitions are compared with that of the relativistic QRPA and Finite Amplitude Method. The accuracy of the global beta decay calculations performed within FRDM+RPA, DF+CQRPA and RHB+QRPA models are analysed.

Keywords: exotic nuclei, isobaric-analog resonances, beta decay, self-consistent approach.

Introduction

The isospin and spin-isospin excitations in charge-exchange reactions and weak interaction processes are the hot topics of nuclear structure theory. The most simpleis the isobaric-analog resonance (IAR), a non-spin excitation ($\Delta L = 0$, $\Delta S = 0$, $\Delta T = 1$) related to the isospin operator τ. If the total spin transferred to the daughter nucleus is non-zero, the Gamow-Teller (GT) giant and pygmy resonances are induced via the spin-isospin operator $\approx \sigma\tau$. The low Exmodes are excited both in charge-exchange reactions and β-decay. This feature is favorable for studying the nuclear structure far from the β-stability line.

The IAR energy is important quantity for determining the nuclear symmetry energy, neutron skin and nuclear matter equation of state (EOS). It is also asensitive indicator of poorly known Coulomb-nuclear correlations strength. A combined analysis of the IAR, β-decay half-lives ($T_{1/2}$) and β-delayed neutron emission probabilities (P_{xn}) helps one to elucidate the isospin and spin-isospin dependent components of nuclear density functional at high isospin-asymmetry regime. Also the β-decay properties are the input parameters for planning the RIB experiments and astrophysical r-process modeling.

The DF+CQRPA [1] calculations of the ground state properties, isobaric-analog resonances and beta-decay properties of nuclei in the vicinity of the neutron shell closures at N = 20, 50, 82 are compared with the spherical relativistic Hartry-Bogolubov plus QRPA model [2] and deformed Finite Amplitude Method (FAM) [3]. All these frameworks include the allowed Gamow–Teller (GT) and first-forbidden (FF) beta decays. An emphasis is made on the quality of density functional in describing the beta decay properties. Special attention is paid to contribution of the first-forbidden transitions (%FF) in total beta-decay rates and delayed multi-neutron emission probabilities.

DF+CQRPA description of the IAR and β-decay properties

Self-consistent models provide microscopically founded extrapolation of the β-decay properties to extreme N/Z ratios important for reliable predictions of beta decay strength function. The most realistic description of the β-decay strength distributions near the closed shells is given by the Interacting Shell-Model including the GT+FF decays [4, 5]. These calculations can be considered as the standard benchmarks for the N = 20, 50, 82 isotones. In a wider region of spherical nuclei including the super heavy ones, an efficient method is the Continuum Quasiparticle Random Phase Approximation (CQRPA) [1] based on the energy-density functional (EDF) approach.

In the DF+CQRPA model, the β-decay strength functions and integral properties are treated within the extended finite Fermi system theory [6] augmented with the self-consistency conditions [7]. For the ground state properties the Fayans EDF [8] is used in which explicit energy dependence arising from an effective account of the many-body correlations is excluded. This results in more sophisticated density dependence than the one of standard Skyrme functional.

The DF+CQRPA model allows for fully self-consistent treatment of the isobaric-analog resonances. The effective interaction in the isospin charge-exchange sector ($\Delta L = 0,\ \Delta S = 0,\ \Delta T = 1$) is derived from the same EDF, as used for finding the single-particle hamiltonian and pairing potential. For simultaneous calculations of the spin-isospin resonances as well as GT and FF beta-decays, the DF+CQRPA model developed in [1] also employs the self-consistent ground states from the same Fayans DF3 functional [8]. As neglecting the spin-isospin dependent components of the DF induce a small error in the ground state properties, for the global beta decay calculations a well-founded spin–isospin effective NN-interaction can be

used instead the one derived from the DF.

Thus, in the DF+CQRPA [1], the Landau-Migdal contact interaction augmented by the finite-range one-π and one-ρ exchange terms modified by nuclear medium [6] is chosen for the one-particle-one-hole (ph) channel. In the ground state calculations, the density-dependent zero-range isovector (T=1) pairing force is used with the A-dependent strength. At the QRPA level, an induced isoscalar (T = 0) proton-neutron effective NN-interaction in the particle-particle channel (dynamic pairing) is assumed to have a similar form. Importantly, the NN-interactions constants are kept the same for all A. The correlations beyond the QRPA are included by re-scaling the spin-dependent multipole operators by the unique energy-independent quenching factor $Q^{1/2} = (g_A/G_A)$. The same factor Q is used for the one-π effective interaction.

The allowed and first-forbidden transitions are treated in terms of the reduced multipole operators depending on the space and spin variables [1]. The full first-forbidden operators set is used. The relativistic operators α, γ_5 are reduced to their space-dependent counterparts via CVC and PCAC relations. This gives a possibility to develop the pnCQRPA on non-restricted ph-base. A provision is added which allows one to fix (before variation) the proper ground state spin-parity in the odd-A isobaric partners.

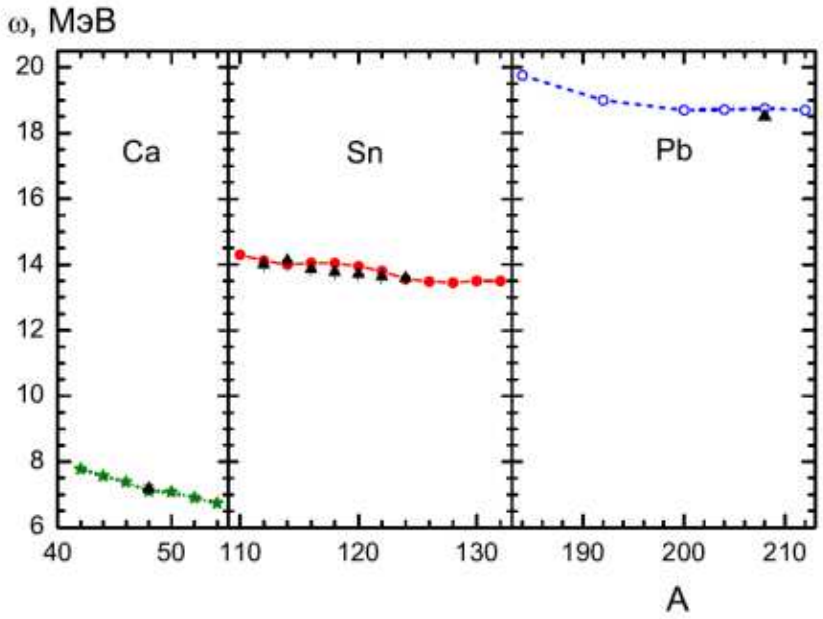

Figure 1. The calculated and experimental IAR energies (relative to the parent ground state) for the Ca, Sn and Pb isotopic chains.

DF+CQRPA description of IAR in Ca, Sn and Pb isotopes

For fully self-consistent description of the IAR several important ingredients have to be included. First, an accurate treatment of the two-body spin-orbit interaction is needed for providing self-consistency. In the present calculations

its parameters are taken the same, as in the FaNDF^0 functional [9]. Second, an important ingredient is the Coulomb interaction. In addition to the direct and Slatter exchange terms, the Coulomb-nuclear correlation (CNC) term [9] is included. If the parameters of CNC are set to provide full screening of the Slatter term, the so-called Nolen-Shiffer anomaly is practically eliminated. Finally, the pairing part of the EDF is chosen to depend on the normal density and its gradient. The DF3f set obtained in such a way from the DF3 functional reduces an underestimate of IAR energy which typically exists in the microscopic models. The deviation of the calculated IAR energies from the reference data in the Ca, Sn and Pb chains (Figure 1) is $\Delta E \leq 200$ KeV.

The Figure 2 shows that only in the fully self-consistent RPA or QRPA, the spread single-particle strengths are collected in a single (degenerate) peak. With no Coulomb exchange included (Figure 2), the IAR energies are too high. Notice that with no dynamic pairing, the Fermi strength function still would have contained spurious satellites with large contribution to the sum rule which is not supported by the (p,n)-type experiments.

Our framework also enables a good description of the neutron matter characteristics, as well as the masses and radii. Thus, no contradiction exist between the estimates for the IAR energies, neutron skin and symmetry energy, as often happened with the Skyrme parametrizations of the EDF [10].

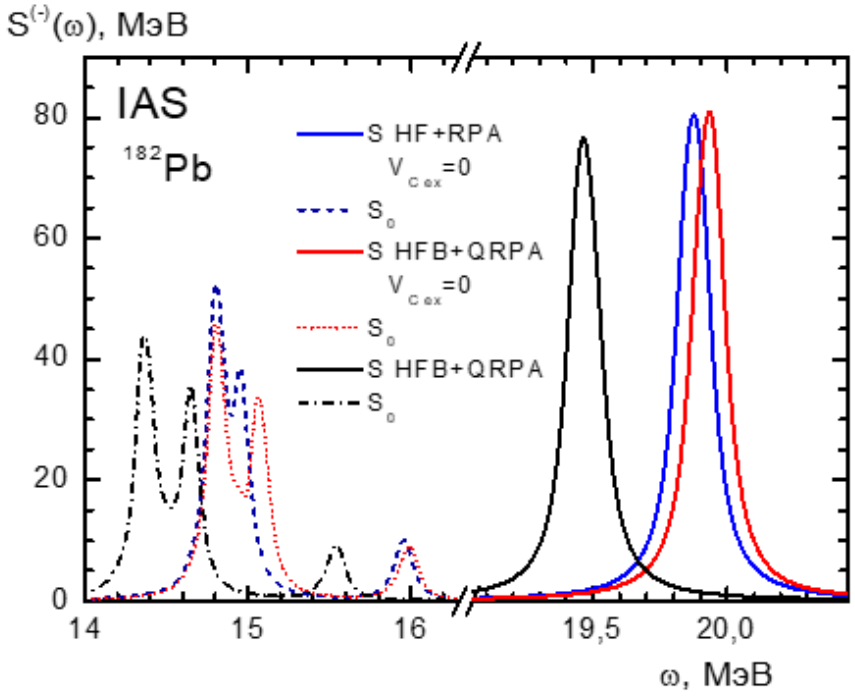

Figure 2. The peaks shown in solid lines are calculated from the HF+RPA (blue), HFB+QRPA(red) without Coulomb exchange and HFB+QRPA with Coulomb exchange (black). The dotted, dash-dotted and dashed lines are the corresponding single-particle responses. (The artificial width of 100 KeV is included for convenience).

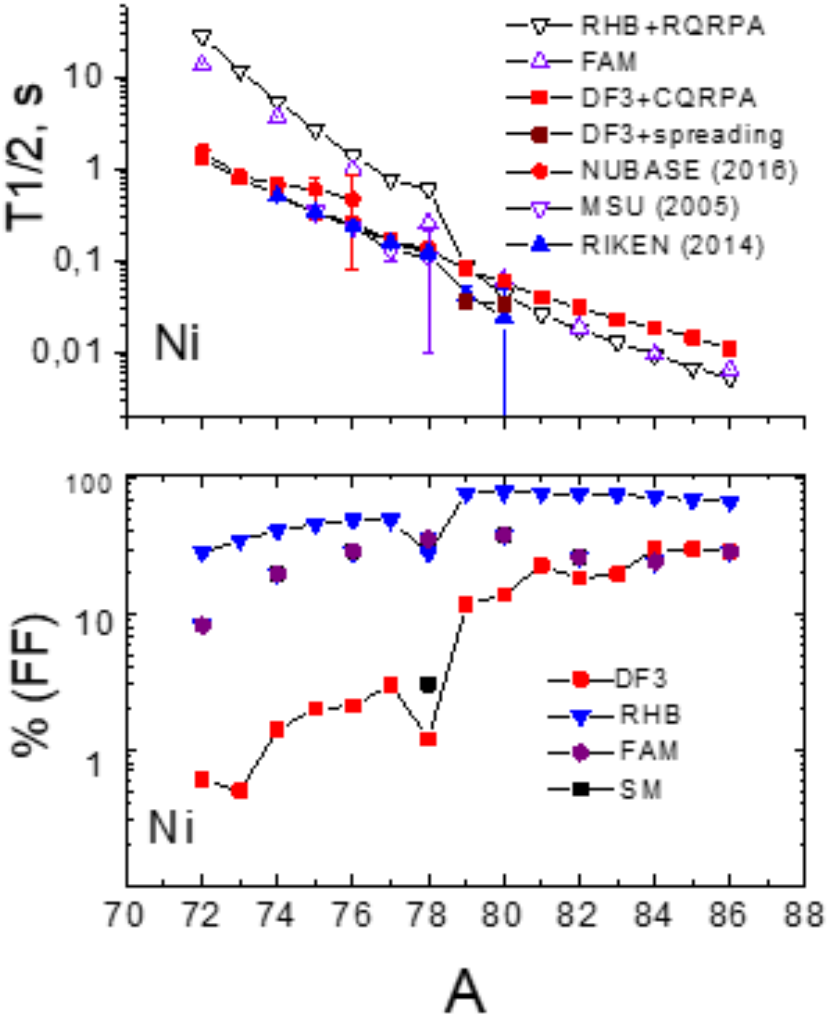

Figure 3. (Top) The experimental half-lives of Ni isotopes from NUBASE-2016, MSU (2005), RIKEN (2014) compared to the theoretical calculations: DF+CQRPA (redsquares),RHB+QRPA [2] (down triangles). (Bottom) The % FF values: DF+CQRPA(red squares), RHB+QRPA [2] (down triangles), FAM [3] (brown squares), Shell Model [4] (black square).

Beta decay half-lives and multi-neutron emission rates

The total half-lives for the reference Ni chain calculated from the DF3+CQRPA [1], RHB+CQRPA [2] and Skyrme+FAM [3] are compared with the experimental data in Figure 3. The latter two calculations significantly overestimate the half-lives for isotopes below the closed neutron shell at N = 50. In the lower panel of Figure 3 we plot the contribution of the first-forbidden transitions to the total decay rates. It shows that below the neutron shell closure N = 50, the contribution of the FF transitions are enhanced in the two models, while the DF3a+CQRPA predicts lower FF contributions relative to the GT ones (this is supported by available decay schemes). Above the neutron shell closure N = 50, the RHB+RQRPA and the DF3a+CQRPA display an increase of the contribution of the FF transitions due to rising occupation of the orbits in the next neutron shell, while the %FF-values in Skyrme+FAM are nearly constant.

Above the closed neutron shell N = 50, the differences in the contributions of

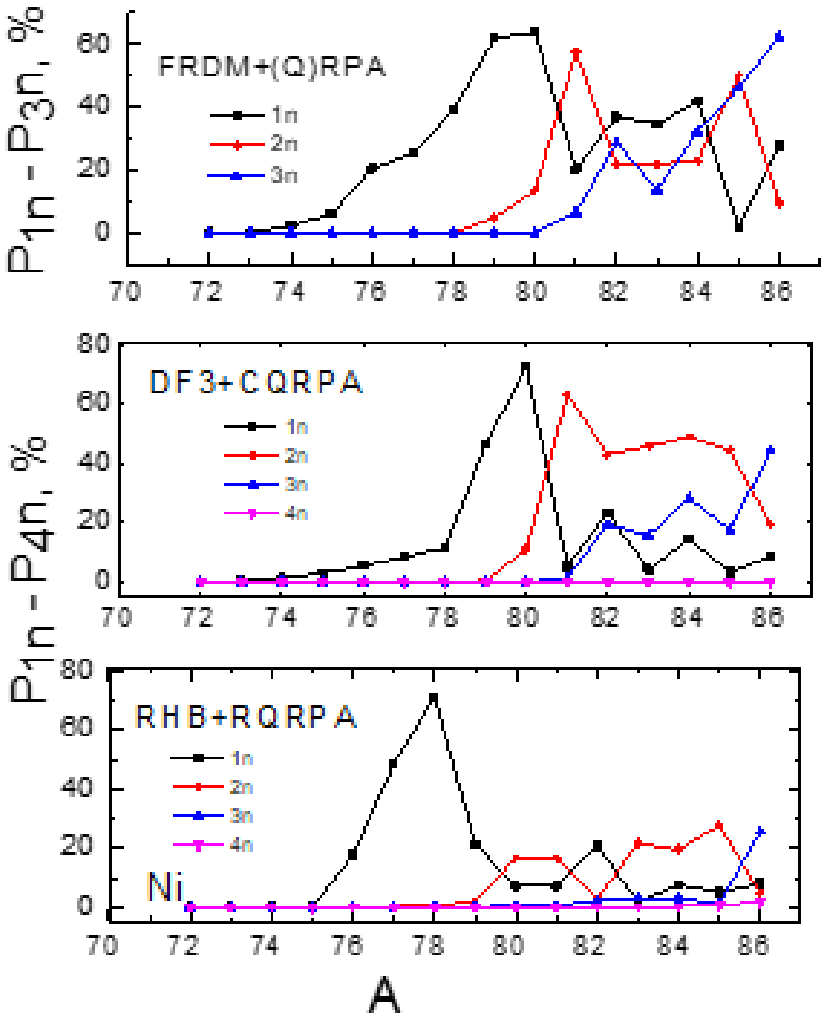

Figure 4. Comparison of beta-delayed neutron emission probabilities of Ni isotopes obtained with three different models: the FRDM [9], DF3+CQRPA [1] and RHB+RQRPA [2].

the first-forbidden transitions are getting smaller and the half-lives predicted by all models are close to each other within their accuracy.

From Figure 4 it can be seen that the P_{xn} values obtained in the FRDM [9] and DF3a+CQRPA [1] are basically similar but differs from the RHB+RQRPA [2]. Namely, the maxima of the one-neutron emission probabilities occur at different masses and P2n-values in the first two models are much higher.

Global calculations of beta decay properties

In Figure 5, the global calculations [1, 11] are compared with the experimental data. The ratio of the half-lives calculated within the spherical CQRPA based on non-relativistic Fayans functional to the experimental data is plotted versus the mass numbers. Here (near-)spherical nuclei in Z = 18-21, 27-35 and 44-51 regions are selected with $T_{1/2}$ ranging from 10 ms to 5 s. The constraint is imposed, as the

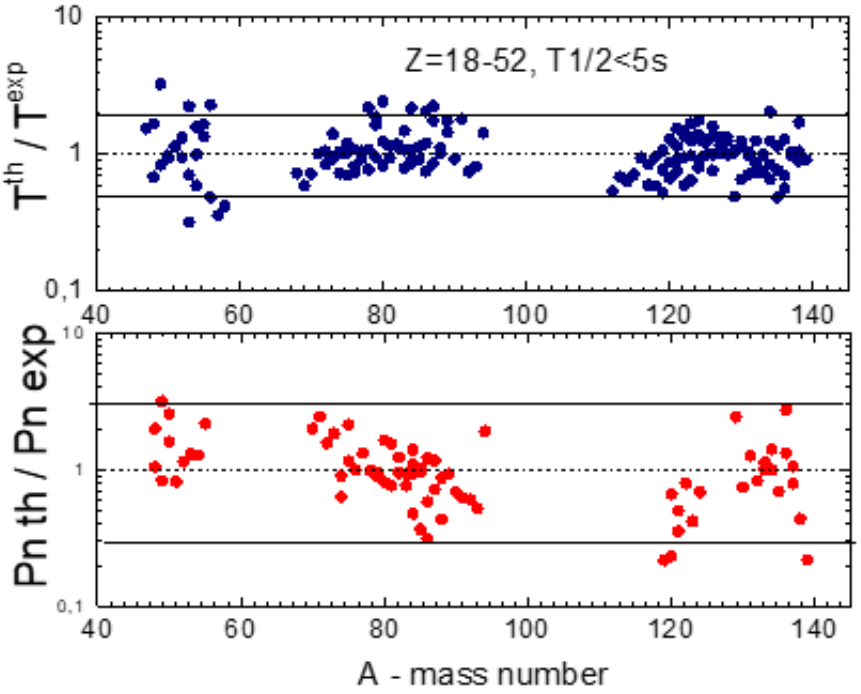

Figure 5. Ratio of theoretical and experimental values of half-lives and P_n -values of (quasi-) spherical nuclei in Z=18-21, 27-35 and 44-51 regions with $T_{1/2} < 5$s calculated using the DF3+CQRPA formalism, plotted versus the atomic number.

formalism employs spherical ground state description. Importantly, it can be seen from Figure 5 that the most of the half-lives are in agreement within the factor of two with the available data.

A similar ratio for the total neutron emission probabilities (P_n) of (near-) spherical nuclei is shown in Figure 4. It can be concluded that experimental data are reproduced basically within the factor of two-three with the exceptions of weakly deformed nuclei in Z = 31-35, A ≈ 85 and Z = 44-45, A ≈ 120 regions with small total P_{tot} - values. In these isotopes non-account for spreading of the beta decay strength due to the interplay of the deformation and complex configurations [12] causes a systematic underestimate of the total P_n -values. Notice that the FRDM [9] describes the half-lives within the factor of 10. The RHB+QRPA [2] describes them mostly within the same accuracy but systematic deviations up to a factor of 100 occur in the regions of nuclear chart between closed shells where the ground state deformations is not weak. For the total P_n -values, the deviations from the data in [9, 2] basically exceed the factor of 10.

Conclusions

The self-consistent approach to nuclear beta-decay allows to reliably describe both ground state properties, as well as isospin and spin-isospin excitations of (quasi)spherical [1, 2, 11] and deformed [3] nuclei in a wide region of the nuclear chart. These self-consistent models based on extended energy density functional are more founded for predicting the β-decay properties than the semi-microscopic approach [9] used as a standard for the r-process modelling.

Reliable description of the Q_β-values, multi-neutron emission thresholds and transition energies are the key to a successful prediction of unknown beta decay properties. The errors in the phase-spaces defined by these quantities impact the beta decay strength distributions propagating further into the half-lives and delayed multi-neutron emission probabilities.

A significant amount of data on very neutron-rich nuclei expected from the new generation radioactive beam facilities can provide a base for verification and further improving of the theoretical predictions. The measurements of the IAR in non-magic stable and unstable nuclei are needed for better constraining the isospin components of the EDF. A simultaneous analysis of the β-decay integral characteristics ($T_{1/2}$, P_{xn}) helps to reconstruct the incomplete β-strength functions.

References

[1] I.N. Borzov, Phys. Rev. C **67** (2003) 025802.
[2] T. Marketin et al., Phys. Rev. C **93** (2016) 025805.
[3] M.T. Mustonen et al., Phys. Rev. C **93** (2014) 014304.
[4] Q. Zhi et al., Phys. Rev. C **87** (2013) 025803.
[5] S. Yoshida et al., Phys. Rev. C. **97** (2018) 054321.
[6] A.B. Migdal, Finite Fermi-system theory (Moscow, 1981).
[7] S.A. Fayans et al., Nucl. Phys. A **676** (2000) 49.
[8] S.A. Fayans, JETP Letters **68** (1998) 169.
[9] P. Moeller et al., Phys. Rev. C **67** (2003) 055802.
[10] Li-Gang Cao et al., Phys. Rev. C **92** (2015) 034308.
[11] I.N. Borzov, Phys. At. Nucl. **81**(6) (2018) 680.
[12] A.P. Severyukhin et al., Phys. Rev. C **90** (2014) 044320.